Novel diagnosis- and progression-related microRNA signatures in melanoma

Helena Gómez-Martínez[1,†], Borja Gómez-Cabañes[1,†], Cristina Galiana-Roselló[1], Alejandro Virués Morales[1], Beatriz Dolader Rabinad [1], Natalia del Rey Díez[1], Adolfo López[1,2], Eva Hernando[3,*], Francisco García-García[1,*]

Affiliations

[1]Computational Biomedicine Laboratory, Principe Felipe Research Centre (CIPF), Valencia, Spain

[2]Joint unit in Biomedical Imaging FISABIO-CIPF, Foundation for the Promotion of Health and Biomedical Research of Valencia Region, Valencia, Spain

[3]Department of Pathology, New York University Grossman School of Medicine, New York, US

[†]These authors contributed equally to this work

Corresponding authors:

Eva Hernando, Eva.Hernando-Monge@nyulangone.org

Francisco García-García, fgarcia@cipf.es

Keywords

Systematic review; meta-analysis; melanoma; transcriptomics; biomarkers; diagnosis; progression; microRNA

ABSTRACT

Melanoma, an aggressive form of skin cancer with a high mortality rate, has recently experienced an increase in incidence. Consequently, the search for biomarkers, such as microRNAs (miRNAs), to facilitate the early detection and management of cancer patients represents a significant current concern.

To identify these potential biomarkers, we developed a novel and integrative strategy. This involved conducting a systematic review of melanoma studies in accordance with PRISMA guidelines, followed by the performance of exploratory analysis and data normalization. Subsequently, individual analyses were conducted for each study, followed by a meta-analysis of miRNAs that integrated all results while considering patient information.

In the diagnostic scenario, we identified twenty-four differentially expressed miRNAs, with eleven being upregulated and thirteen being downregulated. In the severity scenario, a total of twenty-three differentially expressed miRNAs were identified, comprising seven that were upregulated and sixteen that were downregulated. An extensive functional characterization of these miRNA signatures was conducted, providing insight into their biological role and impact on melanoma diagnosis and prognosis.

Our findings contribute to a more comprehensive understanding of the molecular mechanisms and developmental processes involved in melanoma, particularly in early-stage development and ulceration. This, in turn, provides a foundation for the development of novel resources for the precise detection and treatment of melanoma.

INTRODUCTION

Cutaneous melanoma is an aggressive form of skin cancer that has a high propensity for metastasis and is associated with a high mortality rate. It affects the pigment-producing cells on the skin surface and commonly presents with symptoms that include alterations in the cells' size, shape, or color. The prognosis is contingent upon factors such as the thickness of the primary lesion and the timing of diagnosis, which underscores the aggressive nature of melanoma. Indeed, melanoma accounts for approximately 5% of all skin cancers, yet is responsible for 80% of related mortalities, particularly in individuals with fair skin (1-4).

Population-focused awareness campaigns targeting melanoma risks and clinical warning signs facilitate timely access to specialists for diagnosis and treatment. However, despite significant effort, the late onset of symptoms observed in a significant number of patients complicates early detection. Furthermore, the molecular and clinical complexities of melanoma contribute to immune evasion, underscoring the necessity for a comprehensive understanding of biological heterogeneity. In its early stages, cutaneous melanoma remains confined to the epidermis and is typically diagnosed during the radial growth phase. A diagnosis is reached through a combination of morphological analysis and visual examination, with the aid of additional techniques such as lesion dermoscopy and surgical intervention. These approaches have been shown to enhance early-stage survival rates. However, the metastatic potential associated with advanced disease considerably compromises these rates (5-11). The presence of ulceration, defined as skin breakdown over the melanoma lesion, has been identified as a significant predictor of poor clinical outcomes, ranking as the third most important factor in determining survival. It is of the utmost importance to accurately stage the disease and to administer appropriate clinical management, as ulceration has a significant impact on the prognosis of the disease (12).

MicroRNAs (miRNAs) are short non-coding RNAs that regulate the expression of genes associated with numerous biological processes. They often exhibit disease-associated alterations in their expression profiles, which makes them a promising class of biomarkers for cancer diagnosis and prognosis (13-16). miRNA expression profiles frequently become dysregulated during melanoma and other cancer progressions (17, 18), with distinct miRNA species already associated with cervical, breast, prostate, and esophageal cancers (A). Previous studies have indicated that the expression of certain miRNAs, including hsa-miR-193a, hsa-miR-338, and hsa-miR-565, is reduced in BRAF-mutant melanoma. Additionally, low hsa-miR-191 and high hsa-miR-193b expression have been associated with poor survival outcomes (19). Furthermore, hsa-miR-4286 has been shown to influence melanoma cell proliferation and apoptosis by modulating multiple pathways (20). Studying alterations to miRNA expression profiles within melanoma tumor tissue may reveal novel molecular markers for disease diagnosis and progression (20). However, research gaps persist regarding the clinical utility of specific biomarkers for early detection compared with established outcome predictors (21). In this work, we postulated that an integrative computational approach, which evaluates and combines all published datasets on miRNA expression in melanoma, may generate a consensus transcriptomic profile would enhance our comprehension of the underlying molecular mechanisms and regulatory processes, and facilitate the development of innovative strategies for early detection and treatment.

This integrative strategy allowed us to identify two relevant miRNA signatures. The first, focused on diagnosis, included twenty-four differentially expressed miRNAs, with eleven being upregulated and thirteen being downregulated. The second signature was associated with the severity of the disease. This signature comprised twenty-three differentially expressed miRNAs, with seven being upregulated and sixteen being downregulated. Moreover, an exhaustive functional characterization of these miRNA signatures was conducted, shedding light on their biological role and impact on melanoma diagnosis and prognosis.

RESULTS

Systematic review and meta-analysis of miRNA studies

Our systematic review initially identified a total of fifty-four studies from the Gene Expression Omnibus (GEO) and ArrayExpress (AE) databases. In accordance with the established inclusion criteria , seven studies were selected for inclusion in this study (**Figure 1** depicts the complete study selection process).

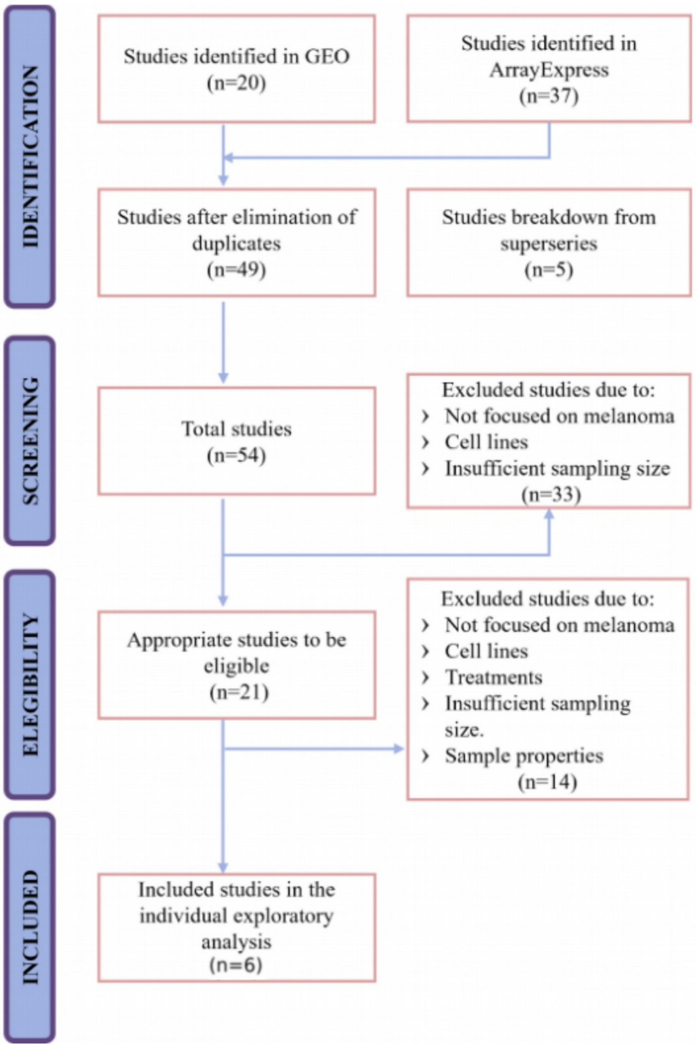
IDENTIFICATION
SCREENING
ELEGIBILITY
INCLUDED
Studies identified in GEO (n=20)
Studies identified in ArrayExpress (n=37)
Studies after elimination of duplicates (n=49)
Studies breakdown from superseries (n=5)
Total studies (n=54)
Excluded studies due to:
› Not focused on melanoma
› Cell lines
› Insufficient sampling size
(n=33)
Appropriate studies to be eligible (n=21)
Excluded studies due to:
› Not focused on melanoma
› Cell lines
› Treatments
› Insufficient sampling size.
› Sample properties
(n=14)
Included studies in the individual exploratory analysis (n=6)

Figure 1. Prisma diagram of the systematic review.

Different potential scenarios related to disease prognosis were considered. These included: i) a diagnostic scenario, which involved a comparison between primary cutaneous melanoma and benign nevi (PM vs. BN); and ii) a severity scenario, which involved a comparison between ulcerated melanoma and non-ulcerated melanoma (UM vs. NUM). The studies included in this research were published between 2010 and 2023 and encompassed a total population of 303 subjects from six studies, with miRNA expression detected in patients' skin tissue samples. The scenarios analyzed and the corresponding number of differentially expressed miRNAs identified per study are summarized in **Tables S1** and **S2**, respectively. Posterior meta-analysis of these expression signatures identified a number of significantly differentially expressed miRNAs in the context of diagnostic and severity scenarios (**Tables 1** and **S3**).

In the diagnostic scenario, a meta-analysis of 1127 miRNAs revealed the presence of 24 differentially expressed miRNAs, comprising 11 that were upregulated and 13 that were downregulated. In the severity scenario, 23 differentially expressed miRNAs were identified from a total of 1327 miRNAs, comprising 7 that were upregulated and 16 that were downregulated. It is noteworthy that miRNAs exhibiting analogous differential expression were identified in both diagnostic and severity scenarios. Specifically, hsa-miR-203 and hsa-miR-205 were found to be downregulated, while hsa-miR-21 was identified as an upregulated miRNA.

Table 1. Results of the meta-analysis of miRNAs for Primary melanoma vs. Benign nevus, and Ulcerated vs. Non-ulcerated. The table shows the names of the miRNAs analyzed, their log fold-change (logFC) and the corresponding adjusted p-value (adjust p-value). Only those miRNAs with an absolute value of logFC greater than 0.5 and adjusted p-value less than 0.05 are included, indicating a significant change in expression.

Primary melanoma vs. Benign nevus			Ulcerated vs. Non-ulcerated		
miRNA	**logFC**	**adjust p-value**	**miRNA**	**logFC**	**adjust p-value**
hsa-miR-1973	3.556	0.0002	hsa-miR-223-3p	1.494	0.0070
hsa-miR-3648	3.340	0.0002	hsa-miR-196b-5p	1.351	0.0370
hsa-miR-3156-5p	3.072	0.0120	hsa-miR-135b-5p	1.262	0.0240
hsa-miR-3911	1.926	0.0040	hsa-miR-363-3p	1.195	0.0210
hsa-miR-21	1.776	0.0002	hsa-miR-451	1.049	0.0001
hsa-miR-3610	1.275	0.0380	hsa-miR-21	0.788	0.0010
hsa-miR-3138	1.274	0.0380	hsa-miR-29a	0.526	0.0390
hsa-miR-3195	1.156	0.0150	hsa-miR-200c	-0.501	0.0020
hsa-miR-3132	0.999	0.0380	hsa-miR-5010-5p	-0.511	0.0480
hsa-miR-142-5p	0.814	0.0020	hsa-miR-301a-5p	-0.515	0.0240
hsa-miR-22	0.754	0.0380	hsa-miR-450a-2-3p	-0.539	0.0390
hsa-miR-23a	-0.561	0.0380	hsa-miR-580-3p	-0.542	0.0480
hsa-miR-30c	-0.579	0.0190	hsa-miR-381-5p	-0.545	0.0400
hsa-let-7d	-0.632	0.0020	hsa-miR-203	-0.561	0.0190
hsa-let-7c	-0.646	0.0380	hsa-miR-487b-5p	-0.590	0.0480
hsa-miR-193b	-0.747	0.0002	hsa-miR-205	-0.593	0.0190
hsa-miR-508-3p	-1.040	0.0002	hsa-miR-552-3p	-0.597	0.0390
hsa-miR-509-3p	-1.305	0.0002	hsa-miR-499a-5p	-0.633	0.0030
hsa-miR-23b	-1.323	0.0002	hsa-miR-518e-3p	-0.649	0.0480
hsa-miR-203	-1.368	0.0160	hsa-miR-489-3p	-0.659	0.0480
hsa-miR-205	-1.571	0.0020	hsa-miR-133a-5p	-0.667	0.0190
hsa-miR-100	-1.700	0.0002	hsa-miR-624-3p	-0.669	0.0480
hsa-miR-101	-1.785	0.0002	hsa-miR-376c-5p	-0.749	0.0260
hsa-miR-211	-1.956	0.0080			

Functional characterization of miRNA target genes

In order to gain insight into the principal functional dynamics of the meta-analyzed miRNAs for each contrast, a gene set enrichment analysis was conducted on their target genes, drawing upon the GO biological processes (GO-BP) and Reactome databases. The diagnostic scenario yielded a total of 15,684 unique target genes, which were subsequently included in the functional analysis. In contrast, the number of unique target genes included in the severity scenario was 20,150.

Biological Process Analysis Unveils Survival Strategies and Microenvironment Adaptation in Primary Melanoma

A GSA on the GO-BP ontology (**Table S4**) was performed based on the complete miRNA-regulated transcriptomic profile. In the context of diagnosis, the fifteen most significantly upregulated GO-BP (**Figure 2A**) comprise mRNA stability and degradation by deadenylation and 3'UTR regulation. Furthermore, metabolic reprogramming, including alterations in glycolysis and the insulin pathway, indicates changes in cellular energy production. Finally, alterations in DNA repair and maintenance, regulation of the G1 phase of the cell cycle, and alterations in cell cycle control suggest altered genomic stability.

Given the considerable number of significantly upregulated GO-BPs, semantic clustering was conducted to comprehensively examine all significantly altered processes and obtain a more complete overview that describes the diagnosis context. The functional clustering yielded the emergence of five distinct clusters, which collectively serve as a functional signature (**Figure 2B**). The largest cluster (**Cluster 1**) centers on the regulation of miRNAs involved in mRNA metabolism and the processing of genetic material at multiple levels—transcriptional, post-transcriptional, and post-translational—highlighting the importance of gene regulation in this context. In accordance with the aforementioned observations pertaining to gene processing, notable alterations at the cell cycle level are noted (**Cluster 4**), particularly at the G2 and G1 DNA damage checkpoints, along with the regulation of the G1/S transition (**Table S4, Cluster 4**). These changes underscore the crucial role of genomic stability, closely tied to apoptotic mechanisms linked to DNA damage and mitochondrial oxidative stress, as illustrated in **Cluster 2**. Additionally, disruptions in growth factor and hormone signaling pathways are noted within this cluster (**Table S4, Cluster 2**). Another significant functional aspect pertains to alterations in differentiation and angiogenesis (**Cluster 3**). This cluster encompasses the modulation of genes implicated in diverse processes of tissue development and morphogenesis processes, as well as processes such as endothelial cell migration within blood vessels, which are pivotal to angiogenesis (**Table S4, Cluster 3**). These tissue remodeling processes are directly related to cellular organization mechanisms (**Cluster 5**), where alterations in the organization of vesicles and nuclei are observed, in conjunction with the organization of membranes and mechanisms of cell adhesion and actin cytoskeleton.

In order to gain a deeper understanding of the interconnections between the upregulated GO-BPs and to identify those of particular significance within the functional landscape, we constructed a similarity network. This approach has yielded a total of eight functional modules, analogous to the clusters obtained by semantic clustering, as illustrated by the colors of the nodes in **Figure 2C**. Two distinct functional modules are identified based on their internal and external connectivity patterns. The “Apoptosis”, “Cell Cycle”, “Protein Phosphorylation”, and “Post-transcriptional Regulation” modules demonstrate a notable degree of internal connectivity, indicative of potential shared biological processes. Furthermore, these categories are interconnected, forming a coherent network with functional interdependence. In contrast, “Response to External Stimuli”, “Protein Organization”, “Adhesion”, and “Development and morphogenesis”, shows a limited number of internal connections and no external connections. This suggests that these categories are more independent, heterogeneous, and isolated functional modules.

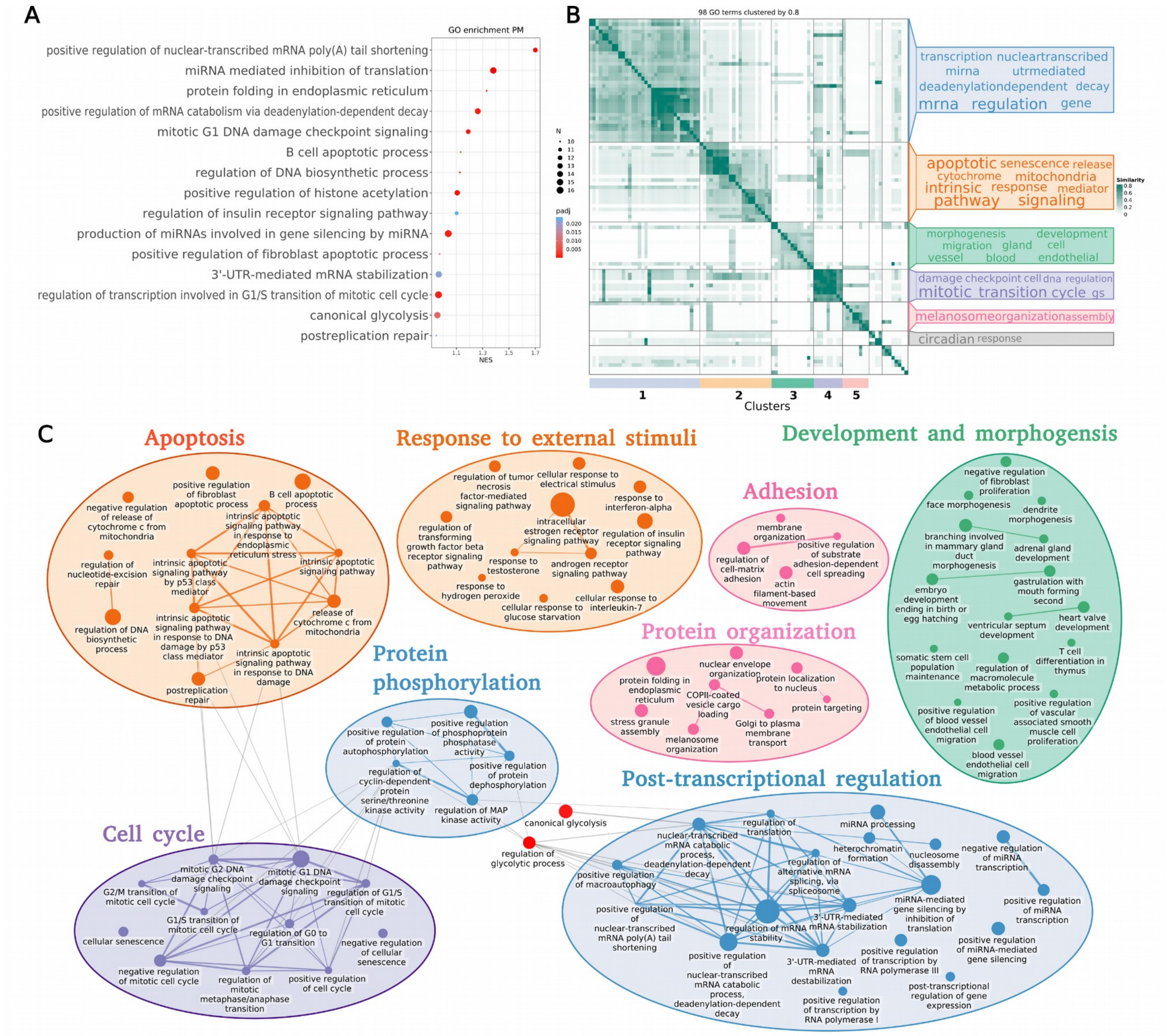

Figure 2. GO-BP enrichment analysis of upregulated miRNAs target genes in primary melanoma. A. Dot plot illustrating the fifteen most significantly altered GO-BPs. The x-axis depicts the degree of enrichment of the various GO-BPs as a function of Normalized Enriched Score (NES), while the y-axis represents the names of the GO-BPs. The color of the dot is indicative of the adjusted p-value and the size indicates the gene set size. **B.** Degree of semantic similarity between significantly altered GO-BPs. Each row and column represents a significant GO term. The green intensity indicates the degree of similarity. The clusters are displayed at the bottom, with the associated word cloud on the right of the plot. **C.** Relationships between GO-BPs terms based on the number of shared genes. Node size is determined by the adjusted p-value, and the width of the edges is determined by the degree of similarity. Each functional module has a representative name and is colored according to the plot B cluster to which the GO-BPs terms belong. GO-BPs with logFC cutoff > 0.5 were included.

Stress-Induced Epithelial Reorganization and Cell Adhesion Disruption through Biological Process Analysis in Ulcerated Melanoma

The functional analysis of the miRNA-regulated genes, comparing ulcerated and non-ulcerated primary melanoma, is illustrated in **Figure S1**. Among the fifteen most significantly upregulated GO-BPs (**Figure S1A**), mRNA stability and metabolism represent the primary altered processes. Additionally, other affected functions include those pertaining to cellular structures and nuclear trafficking, such as adherens junction assembly, cell cycle regulation, DNA damage response, and stress response mechanisms.

A semantic clustering analysis of all significantly upregulated GO-BPs revealed key functional patterns that distinguished between ulcerated and non-ulcerated melanoma (**Figure S1B**). The largest cluster (**Cluster 1**) is primarily concerned with mRNA processing and post-transcriptional modifications, thereby underscoring its central role in gene regulation. The processes of epithelial development and vascularization (**Cluster 2**) are associated with cellular reorganization and protein localization changes (**Cluster 4**), which indicate tissue remodeling. The stress dynamics (**Cluster 3**) encompass responses to both internal stressors, such as ROS and ER overload, and external stressors, including TGF-β, Wnt, insulin, and TNF (**Table S4, Cluster 3**). Apoptotic processes (**Cluster 5**), which involve mitochondrial and DNA damage responses, interact with the stress responses from **Cluster 3**. Minor alterations in cell cycle checkpoints (**Cluster 6**) may potentially influence the process of apoptosis. Lastly, disruptions in cell adhesion (**Cluster 7**), including changes in adherens junctions and integrin interactions with the extracellular matrix (**Table S4, Cluster 7**), are associated with epithelial and cellular changes observed in **Cluster 2** and **Cluster 4**, contributing to ulceration.

A network of similarity was constructed among the upregulated GO-BPs in order to elucidate their biological connections and dynamic changes associated with ulceration (**Figure S1C**). The obtained functional modules are in accordance with expectations based on semantic clustering. Large part of the network plays a central role in genetic information flow, including a critical module on “mRNA stability”, which is linked to “Epigenetic”, “Splicing” or “Telomere organization”. These reflect the functional interdependence between these modules, where alterations in histone, protein phosphorylation, telomeres, and altered transcription and translation suggest adjustments in post-transcriptional and post-translational mechanisms. In consideration of the other network components, a trio of interconnected modules—cell cycle checkpoint regulation ("Cell cycle"), internal stress response ("Stress") and mitochondrial and DNA damage apoptosis ("Apoptosis")—demonstrates the integration of cellular stress responses and their effects on the cell cycle. In combination, the "Cell cycle" and "Protein phosphorylation and ubiquitination" modules interconnection shows the relation between genetic information processing and cellular functions, thereby elucidating intricate pathways in melanoma progression. A module on "Vesicular transport and assembly" demonstrates a close relationship with apoptosis and the stress response, while a smaller module on "Adhesion", including cell and extracellular matrix interactions, highlights the importance of cellular interactions with the microenvironment. Finally, two extensive modules address development, proliferation, and angiogenesis, with a third module, pertaining to "Signaling pathways", include stress responses and receptor signaling associated with growth and developmental stimuli.

Oncogenic Senescence, Rho GTPase Dysregulation, and Altered TGF-β Signaling in Primary Melanoma through Biological Pathway Analysis

We employed Reactome annotation to categorize the pathways that exhibited significant dysregulation across the comparisons (PM vs. BN and Ulcerated vs. Non-Ulcerated). Given the limited number of downregulated results, particular emphasis was placed on the upregulated pathways. The most general and pertinent findings are shown in **Figure 3**, organized as a functional signature with seven blocks. These blocks group the top-level pathways (**Figure 3 right Y-axis**), which are further divided into more specific sub-pathways (**Figure 3 left Y-axis**). Following this hierarchy, we elucidate the frequency distribution of sub-pathways across functional blocks and use the short-hand notation 'Block[top-level pathway]' to indicate the relationship between each block and its sub-pathways. A more comprehensive functional profile at sub-sub-pathway level is detailed for each comparison in **Tables S5** and **S6**.

In light of the results, the functional blocks were defined as follows: 1- genetic information control and processing, 2- metabolic processes, 3- cell signaling and responses, 4- transport and structural organization, 5- cell survival and death, 6- development and maintenance, and 7- immune response (**Figure 3**).

Regarding the Reactome's functional profile in primary melanoma, induced oncogenic senescence (OIS) due to DNA damage is a central issue. Alterations have been identified in the control of cell cycle checkpoints by CDK complexes in response to DNA damage, along with transcriptional regulation of E2F and inhibition of damaged DNA replication by RB1/E2F1 (**Pathways 1[1] and 3[3], Table S5**). Furthermore, alterations are noted in the regulation of the p53 pathway in response to G1 and G2 checkpoints (**Pathways 1[3], Table S5**). These alterations are combined with changes in cell signaling and response to stress (**Pathways 3[2]**), where the regulation of oncogenes such as PTEN or RAF appears to be altered, along with deficiencies in RB1 signaling (**Table S5**). This ultimately results in the activation of OIS, a process that is also influenced by alterations in the stress response (**Pathways 3[1]**). At the metabolic level, alterations are observed in the processes of sumoylation of protein metabolism and capped mRNA processing in RNA metabolism (**Pathways 2[2,3]**). Furthermore, pathways associated with apoptosis show notable disruptions, including regulation of NOS3 metabolism regulation (**Pathways 2[1]**) and BAD activation (**Pathways 5[2], Table S5**) processes being affected. It is also noteworthy that there have been significant alterations in the signaling of cytoskeleton dynamics, cell motility, and adhesion by Rho GTPases are also noteworthy (**Pathways 3[2], Table S5**). Finally, with regard to both cell motility and apoptosis, modifications have been identified in the TGF-B and SMAD signaling pathways, representing the cluster with the largest number of significant alterations (**Pathways 3[2,3]**).

Biological Pathways Underlying in Disrupted Rho GTPase, Tyrosine Kinase Signaling, and Angiogenesis in Ulcerated Melanoma

Reactome pathway analysis reveals several altered biological pathways distinguishing ulcerated from non-ulcerated melanoma. Significant dysregulation in cell cycle regulation and DNA repair pathways, including p53-related mechanisms (**Pathways 1[1,2,3], Table S6**), suggests compromised genomic integrity and an elevated cellular response to DNA damage. This is further accompanied by widespread metabolic disturbances, particularly in lipid, carbohydrate, and amino acid metabolism (**Pathways 2[1]**). Disruptions in protein and RNA metabolism (**Pathways 2[2,3]**) highlight a state of cellular dysfunction, with particular emphasis on stress responses linked to protein folding and SUMOylation, alongside alterations in pathways directly related to cellular stress (**Pathways 3[1], Table S6**).

Ulcerated melanoma shows extensive disruption in signal transduction pathways, particularly through Rho GTPase and receptor tyrosine kinase activation (**Pathways 3[2]**), which may indicate an invasive and metastatic phenotype. This is associated with altered cell-cell communication, extracellular matrix interactions, and death receptor signaling (**Pathways 3[2,3] and 4[3]**), thereby establishing a link between the ulcerative functional response and apoptotic mechanisms, such as anoikis. Moreover, alterations in autophagy, necrosis, and programmed cell death pathways (**Pathways 5[1,2]**) may enhance anoikis resistance and facilitate tumor dissemination. The process of angiogenesis (**Pathways 7[1]**) serves to illustrate the tumor's dependence on neovascularization for growth and metastasis. The dysregulation of immune pathways (**Pathways 7[2]**) indicates the presence of chronic inflammation, immune evasion, and an immunosuppressive microenvironment, which are crucial for melanoma progression and ulceration. These factors are further compounded by alterations in growth factor signaling (**Pathways 3[2,3], Table S6**) and developmental processes (**Pathways 6[2]**), which collectively drive tumor proliferation and progression.

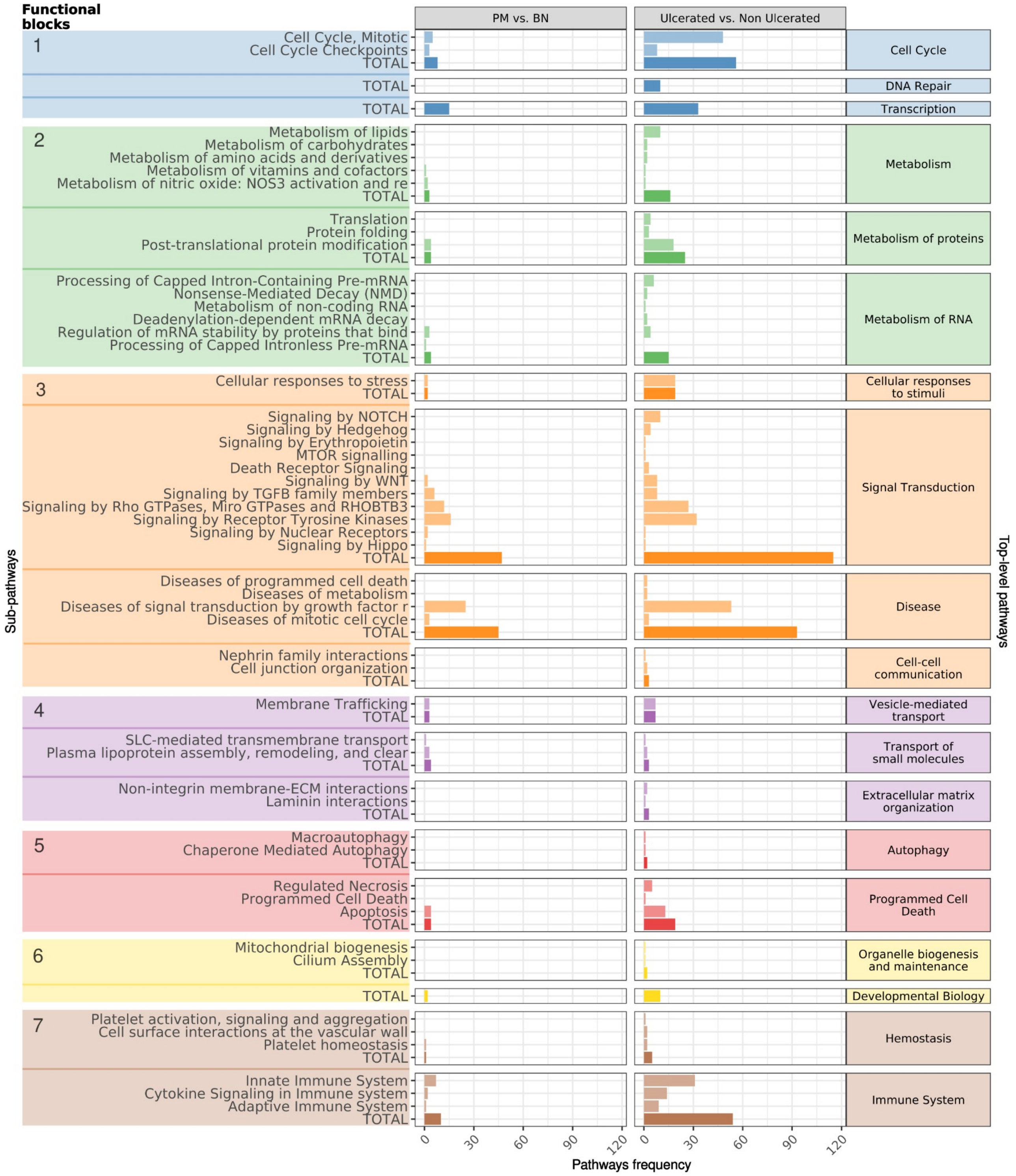

Figure 3. Frequency distribution of significant upregulated Reactome pathways. Using Reactome hierarchical structure, significant pathways have been grouped into top-level pathways (right Y-axis), which are color-coded and ordered by functional blocks. Each top-level pathway is subdivided into more specific sub-pathways (left Y-axis), with a "TOTAL" bar for the sum of significant sub-sub-pathways. The X-axis separates the frequencies for each comparison.

Protein-Protein Interaction Networks of Validated miRNA Target Genes in Melanoma

In order to gain insight into the functional role of miRNAs and their direct impact on melanoma gene regulation, protein-protein interaction (PPI) and regulatory networks have been constructed, including the significant differentially expressed miRNAs and their experimentally validated target genes. In the diagnostic scenario, as the downregulated miRNAs did not yield a connected network, our analysis is limited to the upregulated targets.

Senescence, Migration and Metabolism as Key Regulatory Targets in Primary Melanoma

In the diagnostic scenario, protein-protein interaction (PPI) network analysis revealed a highly interconnected structure consisting of thirty-one genes (p-value: 2.46e-10) forming a single central cluster, which suggests complex interactions between critical genes (**Figure 4A** and **Table S7**). The network revealed three main dynamic regulatory modules: oncogene-induced senescence (**Module 1**), with key genes in the senescence process (e.g., PTEN, ULK1, TP53INP1, CDK6, CCND1, CASP2) and the senescence-associated secretory phenotype (e.g., SOCS1, IL6ST, HIF1AN, HIF1A). Proliferation and epithelial-mesenchymal transition (EMT) (**Module 2**), with genes that play a central role in these processes (e.g., TGFBR2, SMAD3, ZEB1, RAC1) and migration (e.g., ITGAV, ABL2, KIT). Lastly, several genes, including SIRT1, MCL1, ENPP1, BZW1, NFE2L2, and MAT2A represent metabolic reprogramming (**Module 3**). Among the regulated genes, HIF1A, TGFBR2, and SIRT1 are of particular interest due to their central role in their respective functional groups and their active participation in the other exposed regulatory dynamics.

The regulation of these genes by significant miRNAs (**Figure 4B**) illustrated that hsa-miR-142-5p plays a pivotal role in regulatory processes, influencing the regulation of OIS, metabolic reprogramming, and EMT. Other pivotal miRNAs include hsa-miR-3648, hsa-miR-3138, and hsa-miR-3911, which function as central regulators of genes during OIS processes. Moreover, hsa-miR-3911 is involved in the regulation of EMT-related genes, and in conjunction with hsa-miR-3132 and hsa-miR-3156-5p, plays a role in the control of metabolic reprogramming.

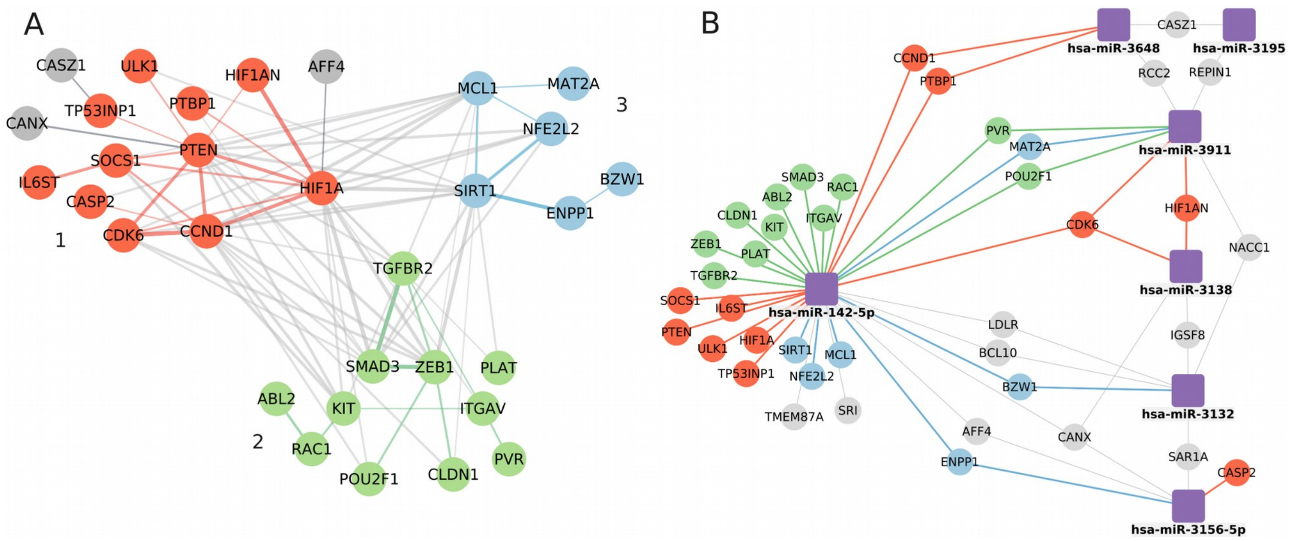
A
CASZ1
ULK1
HIF1AN
AFF4
TP53INP1
PTBP1
CANX
PTEN
SOCS1
IL6ST
HIF1A
CASP2
CDK6
CCND1
1
MCL1
MAT2A
3
NFE2L2
BZW1
SIRT1
ENPP1
TGFBR2
SMAD3
ZEB1
PLAT
ABL2
KIT
ITGAV
2
RAC1
PVR
POU2F1
CLDN1
B
hsa-miR-3648
CASZ1
hsa-miR-3195
CCND1
PTBP1
RCC2
REPIN1
PVR
MAT2A
hsa-miR-3911
POU2F1
SMAD3
RAC1
ABL2
CLDN1
KIT
ITGAV
HIF1AN
CDK6
ZEB1
PLAT
NACC1
TGFBR2
hsa-miR-3138
SOCS1
IL6ST
hsa-miR-142-5p
PTEN
HIF1A
ULK1
SIRT1
MCL1
TP53INP1
NFE2L2
LDLR
BCL10
IGSF8
BZW1
hsa-miR-3132
TMEM87A
SRI
AFF4
CANX
ENPP1
SAR1A
CASP2
hsa-miR-3156-5p

Figure 4. Functional relationships and regulation of upregulated miRNA target genes in primary melanoma. A. PPI network of target genes. Nodes represent genes, while the thickness of the edges indicates the confidence of the interaction. Node colors represent dynamic regulatory modules: 1) Oncogene-induced senescence, 2) Proliferation and epithelial-mesenchymal transition (EMT), and 3) Metabolic reprogramming. Unconnected nodes were excluded. **B.** miRNA-gene regulatory network. Circular nodes correspond to regulated genes, whereas square nodes represent overexpressed miRNAs. Edges represent regulatory relationships. Node colors indicate functional groups represented in network A, whereas gray color refers to unconnected or functionally unrelated nodes.

miRNA Regulates of Cell Cycle, Growth, and Stress Response in Ulcerated Melanoma - Upregulated Gene Networks

A PPI network analysis of the upregulated miRNA target genes revealed the presence of a dense network of 137 genes (p-value: 1.0e-16) in the context of ulceration. These genes were clustered into seven distinct dynamic regulatory modules, with a small subset of genes dominating the connections between them (**Figure 5A** and **Table S8)**.

It is noteworthy that cell cycle genes (e.g., CDK4, CDK6, CDK2, E2F1, CDKN1A, CDKN1B) (**Module 3**) were found to be closely associated with stress response genes (e.g., HIF1A, PTEN, ATM, MDM2, CASP3, BCL2L11) (**Module 1**). The growth and development-related cluster (**Module 2**) comprised a multitude of genes, yet only a select few (e.g., NOTCH1, KRAS, LIF, IGF1R, RUNX2, FOXO1) constituted the majority of the inter-cluster interactions. A comparable pattern was observed in the immune response cluster (**Module 4**), which was distinguished by a high number of internal connections and a limited number of genes (e.g., STAT3, IL6, STAT1, CD8A) that served as links to other clusters. Furthermore, additional peripheral clusters were identified, including those related to cell motility and the cytoskeleton (e.g., ICAM1, SNAI2, STMN1, RDX) (**Module 5**), gene regulation (**Module 6**), and metabolism (**Module 7**).

As illustrated in **Figure 5B**, the regulatory network demonstrates that the majority of genes are predominantly regulated by four dysregulated miRNAs. Among the identified miRNAs, hsa-miR-223-3p has the greatest impact on gene regulation, affecting all described regulatory modules. The peripheral clusters are primarily regulated by hsa-miR-223-3p, with hsa-miR-363-3p also involved in cell motility and cytoskeleton and hsa-miR-196b-5p in gene regulation. A comparable pattern is observed in the immune response cluster, with the exception of hub genes, which are also subject to multiple regulation by hsa-miR-363-3p, hsa-miR-196b-5p, and hsa-miR-135b-5p. In the cell cycle cluster, hsa-miR-363-3p and hsa-miR-196b-5p have been identified as key regulators, in addition to hsa-miR-223-3p. In the case of the stress response and growth-related genes, the regulatory pattern is more uniform, with hsa-miR-196b-5p and hsa-miR-135b-5p playing a pivotal role in growth regulation.

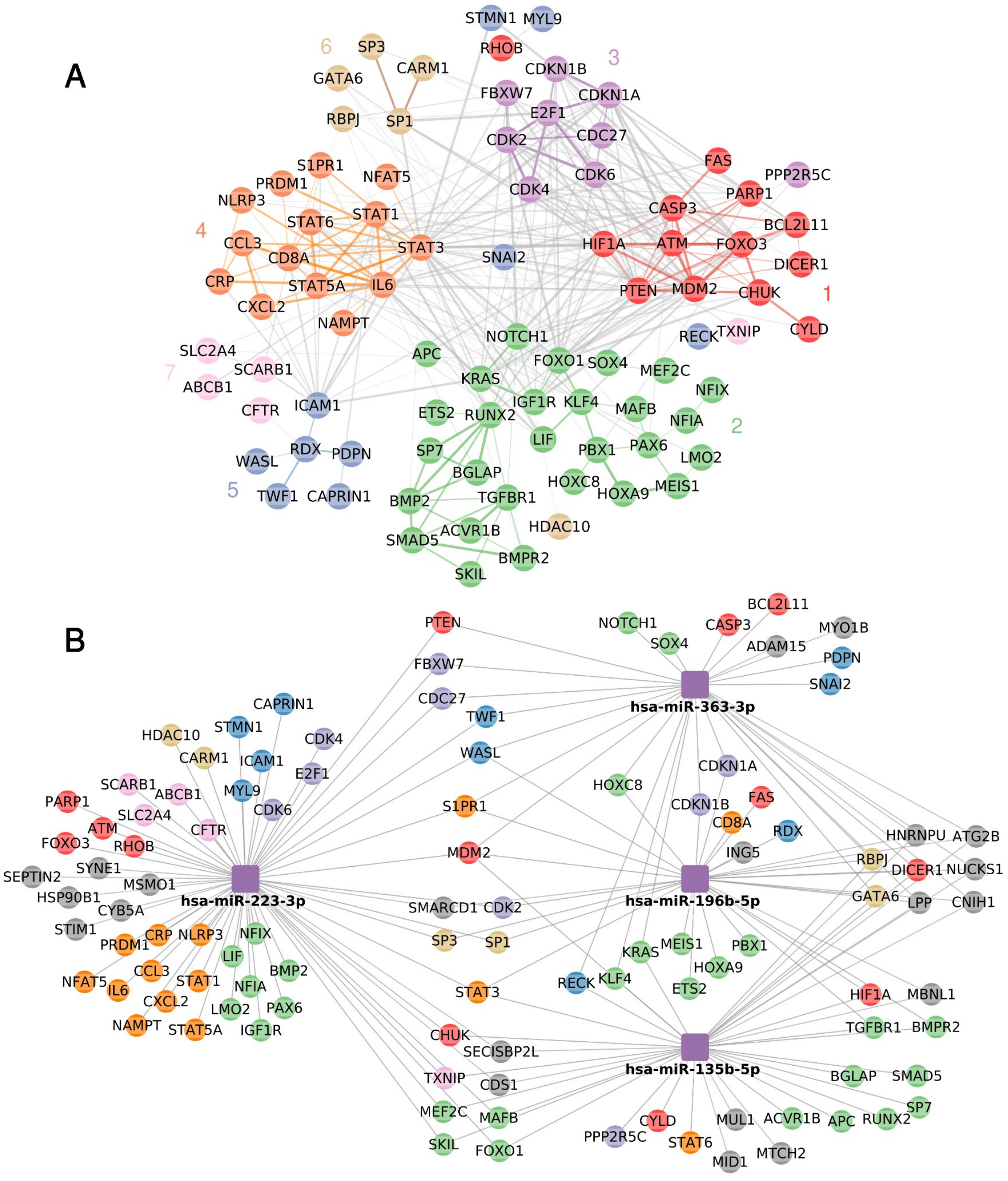
A
STMN1
MYL9
RHOB
6
SP3
CARM1
3
CDKN1B
GATA6
FBXW7
CDKN1A
E2F1
RBPJ
SP1
CDK2
CDC27
S1PR1
FAS
PRDM1
NFAT5
CDK6
PPP2R5C
NLRP3
CDK4
PARP1
STAT1
CASP3
STAT6
BCL2L11
4
CCL3
STAT3
HIF1A
ATM
FOXO3
CD8A
SNAI2
DICER1
CRP
STAT5A
IL6
PTEN
MDM2
CHUK
1
CXCL2
NAMPT
CYLD
NOTCH1
RECK
TXNIP
SLC2A4
APC
FOXO1
SOX4
SCARB1
MEF2C
7
KRAS
NFIX
ABCB1
IGF1R
KLF4
CFTR
ICAM1
ETS2
RUNX2
MAFB
NFIA
2
LIF
RDX
PBX1
PAX6
SP7
PDPN
LMO2
WASL
BGLAP
HOXC8
MEIS1
5
HOXA9
TWF1
CAPRIN1
BMP2
TGFBR1
HDAC10
ACVR1B
SMAD5
BMPR2
SKIL
B
PTEN
NOTCH1
BCL2L11
CASP3
MYO1B
SOX4
ADAM15
FBXW7
PDPN
SNAI2
CDC27
hsa-miR-363-3p
CAPRIN1
TWF1
STMN1
HDAC10
CDK4
CARM1
WASL
ICAM1
CDKN1A
E2F1
SCARB1
HOXC8
ABCB1
MYL9
FAS
PARP1
S1PR1
CDKN1B
SLC2A4
CDK6
CD8A
RDX
ATM
HNRNPU
ATG2B
FOXO3
RHOB
CFTR
ING5
MDM2
RBPJ
SYNE1
DICER1
NUCKS1
SEPTIN2
MSMO1
hsa-miR-196b-5p
HSP90B1
GATA6
LPP
CNIH1
hsa-miR-223-3p
CYB5A
SMARCD1
CDK2
STIM1
CRP
NLRP3
NFIX
PRDM1
SP3
SP1
KRAS
MEIS1
PBX1
LIF
HOXA9
CCL3
BMP2
NFAT5
STAT1
STAT3
RECK
KLF4
ETS2
HIF1A
MBNL1
IL6
NFIA
CXCL2
PAX6
LMO2
TGFBR1
BMPR2
NAMPT
STAT5A
IGF1R
CHUK
SECISBP2L
hsa-miR-135b-5p
TXNIP
BGLAP
SMAD5
CDS1
MEF2C
SP7
MAFB
CYLD
MUL1
ACVR1B
APC
RUNX2
PPP2R5C
STAT6
SKIL
FOXO1
MTCH2
MID1

Figure 5. Functional relationships and regulation of upregulated miRNA target genes in ulcerated melanoma. A. PPI network with node colors indicating dynamic regulatory modules: 1) Stress and Cell Death, 2) Cellular Differentiation and Proliferation, 3) Cell Cycle, 4) Immune System, 5) Mobility and Adhesion, 6) Signal Transduction and Genome Maintenance, and 7) Metabolism. Edges denote intragroup (as node color) or intergroup (gray) connections while thickness indicates the interaction confidence. Unconnected nodes were excluded. **B.** miRNA-gene regulatory

network. Squares represent overexpressed miRNAs; circles represent target genes colored based on panel A. General filters: nodes (min. "Skin" expression of 2/5) and edges (min. 0.6 confidence).

miRNA Influence on Growth and Related Pathways in Ulcerated Melanoma - Downregulated Gene Networks

Similarly, the downregulated scenario yielded a smaller yet similarly high-connected network of fifty genes (p-value: 1.0e-16), as illustrated in **Figure S2A** and **Table S9**. The network of genes regulated by downregulated miRNAs reveals a principal module of growth-related genes (**Module 2**). This module displays a multitude of internal interactions, wherein ERBB2, IGF1R, EGFR, PIK3R2, and SMAD4 serve as connector nodes, linking to pivotal genes involved in cell motility and cytoskeleton (**Module 5**), including SNAI2 and TWIST1. With respect to the cell cycle (**Module 3**), the gene set comprises FOXM1 and CDKN1. In the context of gene regulation (**Module 6**), the ETS1 gene is worthy of particular attention. Ultimately, the cellular response to stress (**Module 1**) demonstrates the involvement of FOXO4 and PDCD4 genes.

As illustrated in **Figure S2B**, the regulatory network reveals notable heterogeneity among the various regulatory modules and miRNAs, underscoring the importance of several key miRNAs. Of these, hsa-miR-489-3p and hsa-miR-499a-5p appear to exert the greatest influence on multiple modules. In particular, hsa-miR-489-3p, in conjunction with hsa-miR-552-3p, hsa-miR-5010-5p, and hsa-miR-133a-5p, serves as a principal regulator of growth-related genes. In addition to the aforementioned hsa-miR-489-3p and hsa-miR-499a-5p, hsa-miR-301a-5p and hsa-miR-624-3p are of considerable importance in gene regulation. In the context of stress response regulation, hsa-miR-489-3p and hsa-miR-499a-5p emerge as key regulators, working in concert with hsa-miR-376c-5p, hsa-miR-301a-5p, and hsa-miR-552-3p.

DISCUSSION

Overall, the results obtained in our integrative strategy propose two novel miRNA signatures: hsa-miR-1973, hsa-miR-3648, hsa-miR-3156-5p, hsa-miR-3911, hsa-miR-3610, hsa-miR-3138, hsa-miR-3195, hsa-miR-3132 or hsa-miR-142-5p for the diagnosis of primary cutaneous melanoma and hsa-miR-223-3p, hsa-miR-196b-5p, hsa-miR-135b-5p, hsa-miR-363-3p, hsa-miR-451, and hsa-miR-29a for the identification of ulcerated primary cutaneous melanoma.

The role of novel miRNA biomarkers in melanoma diagnosis

In the diagnostic scenario, we aimed to identify apparent differences attributed to the disease by comparing melanoma tissue with healthy tissue. We observed the significant alteration of twenty-four miRNAs (eleven upregulated, and thirteen downregulated), which agrees with previous research identifying miRNAs as diagnostic biomarkers for melanoma, including upregulated miRNAs such as hsa-miR-21 (14; 5, (2)), and downregulated miRNAs such as hsa-miR-211, hsa-miR-101, hsa-miR-100, hsa-miR-23b, hsa-miR-193b, hsa-let-7c, hsa-let-7d, hsa-miR-23a, hsa-miR-203, and hsa-miR-205 (reference; 3.; 1; 5.; 2; reference1; reference2). Additionally, our study in the diagnostic scenario also unveiled overexpressed miRNAs with no known association with melanoma diagnosis (e.g., hsa-miR-1973, hsa-miR-3648, hsa-miR-3156-5p, hsa-miR-3911, hsa-miR-3610, hsa-miR-3138, hsa-miR-3195, hsa-miR-3132, and hsa-miR-142-5p). Nevertheless, the significance and robustness of the meta-analysis, alongside validation through various techniques, suggest the importance of the activity of these microRNAs in melanoma, which affect the cell cycle and stress response functions.

The alteration of cell cycle pathways in primary melanoma tissue, particularly affecting processes in the G1/S phase, may involve hsa-miR-1973, which targets *CDK2AP1* and *RAB40C* to impact cell cycle dynamics and protein degradation mechanisms (reference1; Reference2;). hsa-miR-3648 and hsa-miR-142-5p target *CCND1*, with the encoded protein (Cyclin D1) playing a crucial role in cell cycle regulation through the modulation of cyclin-dependent kinases (CDKs) and having implications for poor prognosis in melanoma (Reference 1, Reference, 1; 1; 1). hsa-miR-3911 targets *CDK6*, indicating potential coordination with other miRNAs involved in cyclin regulation (e.g., hsa-miR-3138 and hsa-miR-142-5p). CDK6's significance in melanoma underscores its potential as a therapeutic target, with inhibitors showing promise in reducing tumor growth (Reference1; Reference2; Reference3; Reference4).

hsa-miR-3911 targets the critical cell cycle gene *RCC2*, crucial in cell division, suggesting a role in melanoma recurrence and poor prognosis (1 ;3), and *HIF1AN*, implying a possible downregulation and the subsequent elevation of HIF-1α activity, which can induce the epithelial-to-mesenchymal transition (EMT) in cancer cells and modulate the immune function of tumor cells, potentially facilitating immune evasion ((2; 3; 5 ; (3).). These findings collectively suggest a multifaceted role for miRNA hsa-miR-3911 in melanoma progression and therapy.

We found melanoma to be characterized not only by cell cycle alterations but also by disrupted apoptotic processes. hsa-miR-3648 and hsa-miR-142-5p target the *PTBP1* gene, known to regulate the expression of pyruvate kinase M2 isoform (PKM2) to influence cell proliferation, apoptosis, and metabolism (1;2;3;3). PTBP1's role in tumorigenesis involves apoptosis and cell cycle regulation, with caspase-3 and PARP1 becoming activated upon *PTBP1* downregulation, highlighting its intricate relationship with cancer progression (4; 5). Low *PTBP1* expression correlates with increased susceptibility to caspase-dependent apoptosis in cancer cells (4), promoting melanoma proliferation ((reference1; Reference2; Reference3; Reference4; Reference5; Reference6). Our findings suggest that caspases may play a role in melanoma development as programmed cell death pathways become altered, as evidenced by the upregulation of hsa-miR-3156-5p, which targets the *CASP2* gene, a known tumor suppressor in melanoma (3). While direct mutational inactivation of caspase-2 is unlikely, mechanisms such as miRNA-mediated or epigenetic silencing could explain its reduced expression (3). Our results indicate that hsa-miR-3156-5p may downregulate *CASP2* expression, potentially contributing to failed apoptosis and enhanced melanoma aggressiveness.

The *POU2F1* gene (targeted by hsa-miR-3911 and hsa-miR-142-5p) also alters apoptosis-related processes (Reference1) and affects DNA repair, which may prompt the high burden of somatic mutations in melanoma. The product of the *POU2F1* gene binds to the promoter region of Slc7a11 and regulates melanocytic cell development and progression (1; 2; 3; 5). hsa-miR-3911 and hsa-miR-142-5p also target PVR (the poliovirus receptor), which is overexpressed in many cancers and significantly impacts tumor cell behavior by promoting proliferation (1).

hsa-miR-3132 and hsa-miR-142-5p target *BCL10*, whose encoded protein participates in apoptosis and NF-kappaB (NF-κB) activation (Reference), suggesting a regulatory role in melanoma progression and highlighting possible immune system activation and cellular stress response in melanoma. These findings support the connections between the cell cycle and apoptosis found through the functional enrichment analysis. hsa-miR-3911 and hsa-miR-3132 target *NACC1* (*Nucleus Accumbens-Associated Protein 1*) to increase NF-κB pathway signaling in melanoma cells, indicating a role in cancer progression (reference1; eference2; reference3; reference4; reference5). Regarding hsa-miR-3132, BCL10, and NACC1, this miRNA could have a significant role in NF-κB modulation. On the other hand, downregulation of hsa-miR-3156-5p is linked to JNK pathway activation and reduced JNK levels in various cancers (1). JNK interacts with AFF4, a target of hsa-miR-3156-5p and hsa-miR-142-5p, promoting melanoma cell progression (1). UV light exposure triggers JNK signaling pathway activation (1;2;3;4) and, combined with NF-κB, could support the immune responses and cellular stress associated with melanoma. The immune system represents a key altered pathway in primary melanoma and is influenced by hsa-miR-197 upregulation, which targets *IL17F*, an effector cytokine crucial for innate and adaptive immunity (PubMed:21350122).

Our study in the diagnostic scenario also highlighted functional disruptions related to protein folding within the ER in melanoma, as candidate melanoma biomarkers (hsa-miR-3138, hsa-miR-142-5p, and hsa-miR-3156-5p) target the *CANX* (or *CALX*) gene, which encodes an ER-associated protein involved in protein folding quality control (2 3 4 5). This suggests their potential as robust biomarkers for primary cutaneous melanoma diagnosis. Furthermore, *SAR1A* (targeted by hsa-miR-3156-5p and hsa-miR-3132) plays a critical role in ER homeostasis and COPII vesicle formation, indicating its significance in melanoma pathogenesis (Reference1; reference2; reference3; reference4).

Altered biological processes linked to metabolism and insulin receptors have been observed in primary melanoma. hsa-miR-3156-5p and hsa-miR-142-5p target *ENPP1* (Ectonucleotide Pyrophosphatase/Phosphodiesterase), a glycoprotein with pyrophosphatase and phosphodiesterase activity expressed in various cancer types (1 2 3 5 (3)). *ENPP1* expression in melanoma correlates with poor prognosis (1), while knockdown studies have indicated its potential to reduce metastasis, induce cell death, and enhance tumor responsiveness to immune checkpoint therapy (3). ENPP1's pivotal role in insulin signaling and action further underscores its significance in melanoma pathogenesis and therapy (Reference1; Reference2; Reference3; Reference4). Continuing in this context of altered metabolism and insulin processing, hsa-miR-3138 and hsa-miR-3132 both target *IGSF8*, whose product regulates insulin-like growth factor-I (IGF-I) in melanoma cells, promoting their growth, survival, and migration and the production of the pro-inflammatory cytokine interleukin-8 (IL-8). Both insulin and IGFs represent essential regulators of energy metabolism and growth, and several findings have outlined their role in sporadic malignant melanoma (Reference1; Reference2; Reference3).

Our results also reflected an alteration of lipid metabolic pathways. hsa-miR-3132 and hsa-miR-142-5p target *LDLR* (Low-Density Lipoprotein Receptor), which encodes a protein involved in the uptake of LDL cholesterol from the bloodstream. *LDLR* expression becomes elevated in melanoma and has been related to LDL-mediated cancer growth in mice (4). hsa-miR-3132 and hsa-miR-142-5p algo target *BZW1* ((Basic Leucine Zipper and W2 Domains 1), which encodes a transcription factor that plays a significant role in various cancers, including melanoma (Reference1).

Our results also indicate that biological processes related to genetic information processing, DNA mechanisms, and genetic material biosynthesis become altered in melanoma. hsa-miR-3911 and hsa-miR-142-5p regulate the expression of the gene encoding MAT2A, an enzyme crucial for S-adenosylmethionine (SAM) synthesis, critical metabolite biosynthesis, gene expression regulation, and normal cellular function.

MAT2A becomes downregulated in melanoma and non-small-cell lung cancer (2), which agrees with the findings of our study and suggests that hsa-miR-3911 upregulation may repress *MAT2A*, a synthetic lethal target in cancers with MTAP deletions, found in about 15% of all cancers (4; 5). hsa-miR-3195 and hsa-miR-3648 also have possible implications in genetic information processing as they share the target gene *CASZ1* (Castor Zinc Finger 1), which encodes a protein that plays crucial roles in various biological processes, including multicellular organism development, regulation of transcription, DNA-templating, and regulation of neuron differentiation (reference).

Of note, hsa-miR-3911, hsa-miR-142-5p, hsa-miR-3648, hsa-miR-3132, and hsa-miR-3195 all target one gene - *REPIN1*. This gene encodes the Replication Initiation Region Protein (60kD)(2; 3), which is expressed in melanoma tissue samples (1).

While its role in melanoma remains unclear, hsa-miR-3911 holds promise as a candidate biomarker due to its involvement in various aspects and potential coordination with other miRNAs. Our findings also highlight hsa-miR-142-5p as a potentially exciting biomarker, given its expression in melanocytic tissue and targeting of multiple genes primarily expressed in skin tissue, characteristics shared by other melanoma-associated miRNAs (e.g., hsa-miR-3132, hsa-miR-3648, hsa-miR-3911, hsa-miR-3138, and hsa-miR-3156-5p).

Understanding the miRNA signature in melanoma ulceration

The presence of ulceration in melanoma correlates with unfavorable clinical outcomes and ranks as the third most potent predictor of survival in melanoma patients (reference). We compared ulcerated to non-ulcerated melanoma samples, revealing miRNAs such as has-miR-21, which displays upregulation in both cases and underscores the involvement of this miRNA in melanoma. Upregulated ulceration-associated miRNAs (e.g., hsa-miR-223-3p, hsa-miR-196b-5p, hsa-miR-135b-5p, hsa-miR-363-3p, hsa-miR-451, and hsa-miR-29a) have diverse roles in melanoma and share common target genes, indicating potential coordinated modulation in processes related to melanocytic skin ulceration (e.g., endoplasmic reticulum, apoptosis, cell cycle, cellular stress response, miRNA processing and silencing, or vesicular transport) that also become altered in the diagnostic scenario.

Protein metabolism functions relate to SUMOylation - a post-translational modification in which SUMO proteins become covalently attached to specific lysine residues in target proteins, thereby regulating various aspects of protein function (e.g., transcription, subcellular localization, DNA repair, and cell cycle (reference1; reference2)).

Studies have indicated that malignant melanoma exhibits heightened levels of autophagy, a cellular process involving the digestion of proteins/organelles to generate energy (Reference). Elevated autophagy levels correlate with diminished survival in metastatic melanoma patients, suggesting that autophagy could serve as a prognostic factor and a potential therapeutic target (Reference). Modified expression patterns of autophagy-associated genes (e.g., Beclin1 and LC3) have been observed in ulcerated melanoma, suggesting a plausible connection between autophagy and the aggressive histologic phenotype linked to ulceration (Reference).

As in our study, others have observed the upregulated expression of hsa-miR-223-3p in ulcerated compared to non-ulcerated melanoma (reference). hsa-miR-223-3p targets numerous genes involved in processes altered in ulcerated melanoma and shares target genes with miRNAs implicated in ulcerated melanoma. hsa-miR-196b-5p may have a multifaceted and context-dependent role in cancer biology, acting as an oncogene in melanoma but as a tumor suppressor in other cancer types, warranting further exploration of its mechanisms and potential as a biomarker or therapeutic target (reference; reference2, reference3). Evidence suggests that hsa-miR-135b-5p serves as a cancer type-/context-dependent oncogene or tumor suppressor. The upregulated expression noted in aggressive melanoma subtypes suggests further investigation to clarify the precise role of hsa-miR-135b-5p in melanoma (reference; reference2). hsa-miR-223-3p and hsa-miR-196b-5p both target *MDM2*, whose encoding protein participates in regulating the tumor suppressor protein p53 (overexpression enhances tumorigenisis) (Reference, Reference2).

hsa-miR-223-3p and hsa-miR-196b-5p affect gene silencing processes by targeting *SMARCD1* (also known as

BAF60A), which belongs to the SWI/SNF family of chromatin remodeling complexes and participates in transcriptional activation and repression by chromatin remodeling, which alters DNA-nucleosome interaction to regulate gene expression (Reference).

As in the diagnostic scenario, cell cycle processes also become affected in the ulceration scenario, particularly those regulated by cyclins. hsa-miR-223-3p and hsa-miR-196b-5p target *CDK2*, which encodes a protein essential for the regulation of the G1 to S phase transition alongside cyclin A and E, and the CDK inhibitors p21Cip1 and p27Kip1(Reference). Those both miRNAs algo target SP1 and SP3, two transcription factors that regulate the cell cycle and cell differentiation, SP1 and SP3 are constituents of the Sp family of transcription factors. SP3, involved in cell growth, differentiation, and apoptosis, is a protein-coding gene acting as a transcriptional activator, regulating the expression of target genes (Reference). SP1, also a protein-coding gene, is involved in gene expression regulation, functioning as a transcriptional activator by binding to GC boxes and regulating target gene expression [Reference2]. Despite their similar structures and high homology in DNA-binding domains, SP1 and SP3 exhibit strikingly distinct functions; furthermore, they play crucial roles in the hematopoietic specification, with SP3 partially compensating for SP1 in cells with disrupted SP1 DNA binding (Reference1, Reference2, reference3, reference4).

hsa-miR-223-3p targets *CD27* as does hsa-miR-363-3pb-5p. CD27 remains crucial in regulating T cell immunity, B cell activation, and overall immune system function, with potential implications for cancer immunotherapy (reference). Loss or inactivation of FBXW7 results in the accumulation of oncoproteins such as Cyclin E1, c-Myc, MCL1, mTOR, c-Jun, Notch1, p53, or SNAIL (reference).

hsa-miR-223-3p and hsa-miR-196b-5p share *STAT3* as a target gene with hsa-miR-135b-5p. STAT3 (Signal Transducer and Activator of Transcription 3) - a transcription factor pivotal in cell growth, survival, differentiation, inflammation, immune response, and apoptosis - becomes activated by phosphorylation in response to cytokines and growth factors, leading to dimerization, nuclear translocation, DNA binding, and gene transcription. (reference1; reference2; reference3; reference4; Reference). hsa-miR-223-3p and hsa-miR-135b-5p regulate the gene encoding the RNA binding protein SECISBP2L (Reference). While not directly implicated in melanoma ulceration according to the literature, our results suggest the potential involvement of SECISBP2L, given the association of hsa-miR-223-3p and hsa-miR-135b-5p in ulceration and the fact that RNA binding activity becomes altered in melanoma. We found a comparable situation with *SKIL* and *MAFB*, representing common targets of hsa-miR-223-3p and hsa-miR-135b-5p. SKIL promotes β-catenin signaling and participates in melanoma development; meanwhile, MAFB's exact role in melanoma remains unclear, though expression in melanoma cells and tumor-associated macrophages suggests involvement in relevant cellular processes (reference; reference2).

hsa-miR-223-3p and hsa-miR-135b-5p may influence genome regulation and maintenance by targeting CHUK, a gene crucial to NF-κB signaling, which itself participates in melanoma development (reference). *FOXO1*, targeted by hsa-miR-223-3p and hsa-miR-135b-5p, encodes a tumor suppressor that includes apoptosis in cancer cells; in the context of ulceration, *FOXO1* functions to coordinate keratinocyte responses during wound healing (reference1, reference2). hsa-miR-223-3p and hsa-miR-135b-5p also regulate the *TXNIP* gene, whose downregulation may contribute to melanoma progression by affecting genes related to cell adhesion and the extracellular matrix (Reference). These reports underscore the relevance of these two miRNAs and potentially coordinated gene regulation in melanoma ulceration.

Researchers have also identified and previously implicated downregulated miRNAs in melanoma. Of the miRNAs identified in this study, hsa-miR-499a-5p becomes downregulated in melanoma tissues compared to benign nevi and correlates with poor prognosis, advanced clinical tumor-node-metastasis stage, and lymph node metastasis in melanoma patients (Referencia1, referecia2). Additionally, the MEL38 signature includes hsa-miR-624-3p, contributing to drug/immune resistance in melanoma (reference, reference2)). Moreover, hsa-miR-489-3p inhibits melanoma cell proliferation and glycolytic potential by targeting specific genes involved (reference1; reference2).

In summary, a specific microRNA has not yet been shown as an adequate marker to diagnose and predict the prognosis of melanoma patients; however, our findings underscore the complex regulatory networks orchestrated by miRNAs in melanoma pathogenesis and highlight their potential as diagnostic and therapeutic targets. Notably, we propose an miRNA signature for diagnosis in primary cutaneous melanoma: hsa-miR-1973, hsa-miR-3648, hsa-miR-3156-5p, hsa-miR-3911, hsa-miR-3610, hsa-miR-3138, hsa-miR-3195, hsa-miR-3132 or hsa-miR-142-5p. In addition, we propose the following miRNA-signature for ulcerated primary cutaneous melanoma: hsa-miR-223-3p, hsa-miR-196b-5p, hsa-miR-135b-5p, hsa-miR-363-3p, hsa-miR-451, and hsa-miR-29a. Nevertheless, our observations require further experimental validation, mainly focusing on miRNAs with more significant log fold changes, such as hsa-miR-3648 or hsa-miR-223-3p, to ascertain their clinical relevance and utility.

MATERIALS & METHODS

Systematic review

A systematic review was conducted in accordance with the Preferred Reporting Items for Systematic Reviews and Meta-Analysis (PRISMA) criteria [PMID: 19621072]. A comprehensive search of studies in the Gene Expression Omnibus (GEO) (PMID: 11752295) and Array Express (AE) (PMID: 17132828) repositories was conducted using the keywords: “melanoma”, “microRNAs”, “microRNA” and“miRNA”. The studies were then filtered according to the established inclusion criteria: (i) organism: *Homo sapiens*, (i) dataset type: “Non-coding RNA profiling by array" and “expression profiling by array”. Among the selected studies, we discarded those that met any of the established exclusion criteria: i) studies not focused on melanoma, ii) studies not analyzing miRNAs, iii) studies lacking tissue samples from *Homo sapiens*, iv) minimum sample size (minimum n = 12), v) samples without treatment, and vi) data from cell lines.

Bioinformatic strategy for melanoma biomarkers identification

The bioinformatics workflow (**Figure S3**) was conducted as follows: i) data acquisition, preprocessing, and normalization, and ii) study design and miRNA differential expression analysis for each of the selected studies; iii) miRNA meta-analysis; iv) functional enrichment for miRNA target genes; and v) regulatory study and biological and clinical interpretation..

All data processing was conducted using the R programming language (R Core Team, 2021) from the RStudio graphical interface. The following packages were utilized for data download, processing, and analysis included the following: limma (PMID: 25605792), ggplot2 (Wickham, 2009), dplyr (Wickham, 2023), Biobase (PMID: 25633503), factoextra (Kassambara and Mundt, 2020); impute (Hastie and Tibshirani, 2021), and stringr (Wickham, 2021b).

Data acquisition and preprocessing

All data from the selected studies was downloaded and subjected to individual analysis in order to identify sample groups for the different comparison scenarios. The diagnostic scenario compared primary melanoma versus benign nevi (four studies). The severity scenario compared ulcerated and non-ulcerated primary cutaneous melanoma (four studies). During the analysis, only *Homo sapiens*-specific miRNAs were retained. Subsequently, a descriptive statistical analysis was conducted to identify any anomalous data as well as to assess the distribution of interest groups. After conducting the individual exploratory analysis, the data from the studies were normalized, and standardization was applied to facilitate comparisons between them. Samples showing abnormal behavior were excluded from further analysis. This process ensured that all selected studies started with normalized data, minimizing the risk of introducing new biases and reducing variability in subsequent analyses.

miRNA differential expression and meta-analysis

A differential expression analysis of miRNAs was conducted for each study individually using the limma R package. Comparisons were made between the various groups delineated in the preceding section. The control group consisted of benign nevi, non-ulcerated melanoma cases, and living patients in each corresponding scenario. Two meta-analyses were conducted, one for each scenario, using the R package metafor (Viechtbauer, 2010) under the DerSimonian & Laird random-effects model (PMID: 3802833). This model accounts for the inherent variability of individual studies by assigning greater weight to studies with less variability when computing meta-analysis results. Consequently, the most robust miRNAs between studies are identified. P-values, corrected p-values, logFC, logFC standard error (SE), and logFC 95% confidence intervals (CI) were calculated for each evaluated miRNA. miRNAs with adjusted p-values lower than 0.05 and absolute logFC higher than 0.5 were considered significant.

Functional characterization of miRNAs targets genes

To gain a deeper insight into the biological functions of the different scenarios, the targets of the total miRNAs included in each meta-analysis were identified using TarBase v8.0 [Ref] and miRTarBase v9.0 [Ref], which exclusively provide experimentally validated miRNA targets. Subsequently, a Gene Set Analysis (GSA) was performed on the Gene Ontology (GO) [Ref] database and the REACTOME [Ref] database using the logistic regression model implemented in the mdgsa R package [Ref] (version 0.99.2). First, a list of ranked miRNAs was created using the associated p-value and log fold change (logFC). Subsequently, mdgsa enables the transfer of ranking index information from miRNAs to their target genes, thus facilitating the inference of gene regulation levels from miRNA differential expression levels. The functional annotations were retrieved via the biomaRt package (version 2.50.3) [Ref] for the GO database and the Reactome.db package (version 1.77.0) [Ref] for the REACTOME database. The results were adjusted using the Benjamini-Hochberg (BH) [Ref] method, and significance was determined with an adjusted p-value of less than 0.05. In the context of a diagnostic scenario, terms exhibiting an absolute logFC exceeding 0.5 were deemed to be significantly enriched. In the severity scenario, a stricter cutoff of 0.75 was implemented due to the high number of results. These adjustments were essential for managing the complexity of the data and focusing the analysis on the most biologically relevant and impactful terms. simplifyEnrichment package (version 1.10.0) [Ref] was used to cluster and simplify the GO functional results. To explore the similarity relationships between the altered GO terms we used REVIGO [Ref], allowing us to visualize them through a network. The analysis was conducted with the Homo sapiens database, using SimRel similarity measure, a result size of 0.9 to ensure that only highly redundant GO terms were removed, and adjusted p-values for ranking. Subsequent visual adjustments were made using Cytoscape (version 3.10.1) [**REF**].

miRNA-target gene interactions

For a more specific analysis, only the significant miRNAs in each scenario were selected, and the corresponding target genes were identified (**Table S11**). Three critical filtering criteria were applied to refine the validity of miRNA-target interactions: i) targets with 'strong evidence' of validation, which includes reporter assays, Western blot, and qPCR (as documented in miRTarBase) and targets that received at least three validations categorized under 'less strong evidence,' ii) targets regulated by multiple significant miRNAs, regardless of the type of validation, iii), implementing a gene expression filter utilizing stringApp [Ref] to discard target genes not exhibiting a minimum expression level of 2 out of 5 in skin tissue. This additional criterion ensured relevance and specificity to the physiological context. The final selection of genes was employed to construct a PPI network, integrating high-confidence, experimentally validated, and biologically relevant interactions tailored to each scenario using the Cytoscape software. In conjunction with this approach, a miRNA-target gene relationship network was constructed using Cytoscape software to visualize the regulatory dynamics and interactions for each comparison between significant miRNAs and their targets after applying the critical filtering criteria.

CONFLICT OF INTEREST

All the authors declare no conflict of interest.

ACKNOWLEDGEMENTS

The authors thank the Principe Felipe Research Center (CIPF) for providing access to the cluster, co-funded by European Regional Development Funds (FEDER) in the Valencian Community 2014-2020. The authors also thank Stuart P. Atkinson for reviewing the manuscript.

This research was supported by and partially funded by the Institute of Health Carlos III (project IMPaCT-Data, exp. IMP/00019), co-funded by the European Union, European Regional Development Fund (FEDER, "A way to make Europe"), and PID2021-124430OA-I00 funded by MCIN/AEI/10.13039/501100011033/

FEDER, UE ("A way to make Europe"). Borja Gómez-Cabañes is supported by a PhD fellowship funded by the Spanish Association Against Cancer in Valencia (PRDVA234163GOME).

DATA AND CODE AVAILABILITY

The data used for the analyses described in this work are publicly available at GEO and AE repositories [Ref and Ref]. The accession numbers of the GEO datasets downloaded are GSE18509, GSE34460, GSE59334, GSE62370, GSE62371, GSE211090, and GSE211092. The accession number of the AE datasets downloaded is EMTAB4915.

The code developed for the analyses described in this work has been publicly available at Zenodo (https://github.com/adlpecer/PD_GeneMetaanalysis). All software and versions are detailed in **Additional file 2: Table S10**.

AUTHOR CONTRIBUTIONS STATEMENT (CRediT-compliant)

Conceptualization: EH, FGG; Data Curation: HGM, BGC; Investigation: EH, FGG, CGR, HGM, AVM, BDR, NRD, BGC; Supervision: EH, FGG, ALC; Writing-Original Draft Preparation: EH, FGG, CGR, HGM, AVM, BDR, NRD, BGC; all authors read and approved the final manuscript.

REFERENCES

1. Ambros V. microRNAs: tiny regulators with great potential. Cell. 2001;107(7):823–6
2. Atkins MB, Curiel-Lewandrowski C, Fisher DE, Swetter SM, Tsao H, Aguirre-Ghiso JA, et al. The State of Melanoma: Emergent Challenges and Opportunities. Clin Cancer Res. 2021;27(10):2678–97
3. Balch CM, Gershenwald JE, Soong S-J, Thompson JF, Atkins MB, Byrd DR, et al. Final version of 2009 AJCC melanoma staging and classification. J Clin Oncol. 2009;27(36):6199–206
4. Bartel DP. MicroRNAs: genomics, biogenesis, mechanism, and function. Cell. 2004;116(2):281–97
5. Caramuta S, Egyházi S, Rodolfo M, Witten D, Hansson J, Larsson C, et al. MicroRNA expression profiles associated with mutational status and survival in malignant melanoma. J Invest Dermatol. 2010;130(8):2062–70
6. Erdei E, Torres SM. A new understanding in the epidemiology of melanoma. Expert Rev Anticancer Ther. 2010;10(11):1811–23
7. Fares J, Fares MY, Khachfe HH, Salhab HA, Fares Y. Molecular principles of metastasis: a hallmark of cancer revisited. Signal Transduct Target Ther. 2020;5(1):28

8. Gaur A, Jewell DA, Liang Y, Ridzon D, Moore JH, Chen C, et al. Characterization of microRNA expression levels and their biological correlates in human cancer cell lines. Cancer Res. 2007;67(6):2456–68
9. Goyal M, Knackstedt T, Yan S, Hassanpour S. Artificial intelligence-based image classification methods for diagnosis of skin cancer: Challenges and opportunities. Comput Biol Med. 2020;127:104065
10. He L, Hannon GJ. MicroRNAs: small RNAs with a big role in gene regulation. Nat Rev Genet. 2004;5(7):522–31
11. Jayawardana K, Schramm S-J, Tembe V, Mueller S, Thompson JF, Scolyer RA, et al. Identification, Review, and Systematic Cross-Validation of microRNA Prognostic Signatures in Metastatic Melanoma. J Invest Dermatol. 2016;136(1):245–54
12. Kaiser S, Vassell R, Pinckney RG, Holmes TE, James TA. Clinical impact of biopsy method on the quality of surgical management in melanoma. J Surg Oncol. 2014;109(8):775–9
13. Kirstein JM, Hague MN, McGowan PM, Tuck AB, Chambers AF. Primary melanoma tumor inhibits metastasis through alterations in systemic hemostasis. J Mol Med (Berl). 2016;94(8):899–910
14. Komina A, Palkina N, Aksenenko M, Tsyrenzhapova S, Ruksha T. Antiproliferative and Pro-Apoptotic Effects of MiR-4286 Inhibition in Melanoma Cells. PLoS One. 2016;11(12):e0168229
15. Mueller DW, Rehli M, Bosserhoff AK. miRNA expression profiling in melanocytes and melanoma cell lines reveals miRNAs associated with formation and progression of malignant melanoma. J Invest Dermatol. 2009;129(7):1740–51
16. Naik PP. Cutaneous Malignant Melanoma: A Review of Early Diagnosis and Management. World J Oncol. 2021;12(1):7–19
17. Neagu M, Constantin C, Tanase C. Immune-related biomarkers for diagnosis/prognosis and therapy monitoring of cutaneous melanoma. Expert Rev Mol Diagn. 2010;10(7):897–919
18. Nirschl CJ, Suárez-Fariñas M, Izar B, Prakadan S, Dannenfelser R, Tirosh I, et al. IFNγ-Dependent Tissue-Immune Homeostasis Is Co-opted in the Tumor Microenvironment. Cell. 2017;170(1):127-141.e15
19. O'Shea SJ, Rogers Z, Warburton F, Ramirez AJ, Newton-Bishop JA, Forbes LJL. Which symptoms are linked to a delayed presentation among melanoma patients? A retrospective study. BMC Cancer. 2017;17(1):5
20. Sandru A, Voinea S, Panaitescu E, Blidaru A. Survival rates of patients with metastatic malignant melanoma. J Med Life. 2014;7(4):572–6
21. Swetter SM, Tsao H, Bichakjian CK, Curiel-Lewandrowski C, Elder DE, Gershenwald JE, et al. Guidelines of care for the management of primary cutaneous melanoma. J Am Acad Dermatol. 2019;80(1):208–50